Enhanced respiration prevents drug tolerance and drug resistance in *Mycobacterium tuberculosis*

Catherine Vilchèze[a,b], Travis Hartman[b], Brian Weinrick[a,b], Paras Jain[b], Torin R. Weisbrod[b], Lawrence W. Leung[c], Joel S. Freundlich[d], and William R. Jacobs Jr.[a,b,1]

[a]Howard Hughes Medical Institute, Albert Einstein College of Medicine, Bronx, NY 10461; [b]Department of Microbiology and Immunology, Albert Einstein College of Medicine, Bronx, NY 10461; [c]Gray Box Biology LLC, New York, NY 10027; and [d]Department of Medicine, Center for Emerging and Reemerging Pathogens, New Jersey Medical School, Newark, NJ 07103

Contributed by William R. Jacobs Jr., March 17, 2017 (sent for review October 7, 2016; reviewed by Courtney C. Aldrich, Meindert H. Lamers, and Alan Sher)

Persistence, manifested as drug tolerance, represents a significant obstacle to global tuberculosis control. The bactericidal drugs isoniazid and rifampicin kill greater than 99% of exponentially growing *Mycobacterium tuberculosis* (*Mtb*) cells, but the remaining cells are persisters, cells with decreased metabolic rate, refractory to killing by these drugs, and able to generate drug-resistant mutants. We discovered that the combination of cysteine or other small thiols with either isoniazid or rifampicin prevents the formation of drug-tolerant and drug-resistant cells in *Mtb* cultures. This effect was concentration- and time-dependent, relying on increased oxygen consumption that triggered enhanced production of reactive oxygen species. In infected murine macrophages, the addition of *N*-acetylcysteine to isoniazid treatment potentiated the killing of *Mtb*. Furthermore, we demonstrate that the addition of small thiols to *Mtb* drug treatment shifted the menaquinol/menaquinone balance toward a reduced state that stimulates *Mtb* respiration and converts persister cells to metabolically active cells. This prevention of both persister cell formation and drug resistance leads ultimately to mycobacterial cell death. Strategies to enhance respiration and initiate oxidative damage should improve tuberculosis chemotherapies.

drug resistance | mycobacterial persister | oxygen consumption | thiol

Multidrug-resistant tuberculosis (MDR-TB) and extensively drug-resistant tuberculosis (XDR-TB) have become major threats to global public health (1). The emergence of MDR- and XDR-TB has been attributed primarily to the lengthy, 6-mo TB treatment. Failure to complete a full course of treatment can lead to the development of drug resistance and relapse, which requires up to 2 y to treat.

Resistance to the first-line TB drug isoniazid (INH) is most often a result of mutations in *katG*, which encodes a catalase peroxidase, the activator of INH (2), but other genes have also been associated with INH resistance in TB (3). In particular, genes involved in the biosynthesis of mycothiol, the main reducing thiol in mycobacteria and a storage molecule for cysteine (4), have been implicated in resistance to INH and the second-line TB drug ethionamide (ETH) in mycobacteria (5–8). We sought to explain the mechanisms by which mutations in the *mshA*-encoded glycosyltransferase, the first step in mycothiol biosynthesis, leads to a defect in mycothiol production and INH or ETH resistance in *Mycobacterium tuberculosis* (*Mtb*) (9). We hypothesized that mycothiol-deficient *mshA* mutants accumulated cysteine, leading to drug resistance, but surprisingly, we found that the addition of cysteine to INH-treated *Mtb* sterilized the cultures. In this report, we present the effects of adding cysteine to drug-susceptible and drug-resistant *Mtb* strains treated with INH. We performed a comprehensive analysis of the transcriptome, metabolites, production of reactive oxygen species (ROS), and cellular respiration to propose that sterilization of *Mtb* cultures can be obtained by coercing *Mtb* into a constant active metabolic state that renders the bacteria continuously susceptible to the cidal effects of the TB drugs.

Results

Addition of Cysteine to INH-Treated, Exponentially Growing Cultures of *Mtb* Results in Sterilization of Drug-Susceptible and Drug-Resistant *Mtb*. Treatment of *Mtb* H37Rv cultures with INH in vitro is a triphasic event starting with a rapid initial killing of *Mtb* cells, followed by a stagnation step where the persister population is revealed, and finally the emergence of INH-resistant bacteria (10). Low-level INH resistance was previously observed in *Mtb* mutants that failed to produce mycothiol (9), a cysteine reservoir, leading us to hypothesize that these mutants might accumulate cysteine and that this accumulation mediated INH resistance. To test this hypothesis, increasing concentrations of cysteine (from 8 μM to 4 mM) were added to INH-treated *Mtb* H37Rv cultures. Rather than conferring INH resistance, the increasing concentrations of cysteine caused increasing delays in the growth of INH-resistant mutants (Fig. S1*A*), with their appearance completely inhibited at the highest concentration of cysteine tested (4 mM). Surprisingly, the combination of 4 mM of cysteine and INH had sterilized the culture (Fig. 1*A*). Both INH and the combination of INH and cysteine (INH/Cys) generated the same kinetics of killing for the first 7 d, but then the survival patterns with the two treatments diverged (Fig. 1*A*). Bacterial counts after 3 wk of INH/Cys treatment ranged between 0 and 10 CFU/mL, representing a 6-log killing of the initial culture (Fig. 1*A*), and none of these residual colonies were INH-resistant. This increased killing was not a result of a bactericidal effect of cysteine itself, because growth and viability of *Mtb* were not affected by the addition of cysteine alone, nor was the outcome specific to *Mtb* H37Rv; the same sterilizing activity was observed when either *Mtb* Beijing or *Mtb*

Significance

Tuberculosis (TB) patients would greatly benefit from shorter treatment options. The treatment of drug-susceptible TB, a disease caused by the bacillus *Mycobacterium tuberculosis*, is a lengthy and strenuous process. This long therapy is because of the ability of a small population of cells to become drug-tolerant. Here, we demonstrate that the addition of small thiols to drug-treated *M. tuberculosis* prevents the emergence of drug-tolerant but also drug-resistant cells leading to sterilization of the cultures in vitro. The thiols potentiate drug activity by preventing the cells from entering a persister state and shutting down their metabolism while generating an oxidative burst. This dual mechanism of killing could lead to novel approaches to shorten TB chemotherapy.

Author contributions: C.V. and W.R.J. designed research; C.V., T.H., B.W., P.J., T.R.W., and L.W.L., performed research; J.S.F. contributed new reagents/analytic tools; C.V., T.H., B.W., P.J., T.R.W., L.W.L., and W.R.J. analyzed data; and C.V. and W.R.J. wrote the paper.

Reviewers: C.C.A., University of Minnesota; M.H.L., Medical Research Council; and A.S., National Institute of Allergy and Infectious Diseases.

The authors declare no conflict of interest.

Data deposition: The data reported in this paper have been deposited in the Gene Expression Omnibus (GEO) database, https://www.ncbi.nlm.nih.gov/geo (accession no. GSE86184).

[1]To whom correspondence should be addressed. Email: jacobsw@hhmi.org.

This article contains supporting information online at www.pnas.org/lookup/suppl/doi:10.1073/pnas.1704376114/-/DCSupplemental.

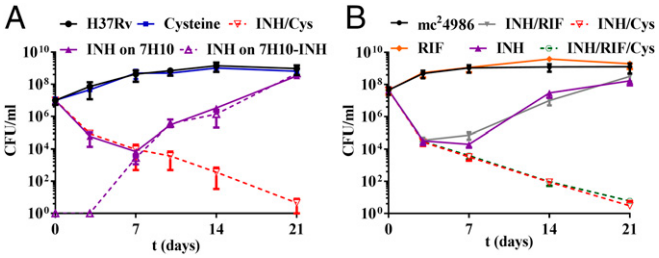

Fig. 1. The combination INH/Cys sterilizes drug-susceptible and drug-resistant *Mtb* cultures. (*A*) Viability of *Mtb* treated with INH (7.3 μM, 20 times the MIC), cysteine (4.0 mM), or INH/Cys. The INH-treated culture was plated on 7H10 plates and 7H10-INH plates containing 3.7 μM of INH. (*B*) The RIF-resistant strain mc²4986 (*Mtb* H37Rv *rpoB* H445R) was treated with RIF (1.2 μM), INH (7.3 μM), cysteine (4.0 mM), or a combination. The combinations used the same concentrations as the individual treatments. Aliquots were taken at indicated times and plated to determine CFUs. Average with SD is plotted (n = 2–4).

CDC1551 was treated with INH/Cys (Fig. S1 *B* and *C*). Interestingly, the growth inhibition of *Mtb* by INH/Cys was observed only when cysteine was added at the same time or no more than 1 d following the addition of INH (Fig. S1*D*).

Next, we investigated the possibility that INH/Cys might be beneficial for drug-resistant TB therapy by treating a rifampicin (RIF)-resistant *Mtb* strain (mc²4986, H37Rv *rpoB* H445R) with INH, cysteine, and INH/Cys (Fig. 1*B*). INH/Cys with or without the addition of RIF prevented the growth of drug-resistant populations and reduced the bacterial population by 6-log after 3 wk, similar to our observations with drug-susceptible *Mtb* strains.

A Free Thiol Group Is Required in Combination with INH for Sterilizing Activity. To determine whether the observed sterilization activity of the INH/Cys combination was cysteine-specific, other thio-compounds or structurally similar amino acids were added to INH-treated *Mtb* cultures and the growth of the cultures was followed visually. The emergence of a growing population after 14 d was prevented only when *Mtb* was treated with a combination of INH and a compound having a free thiol group (Table S1). Interestingly, in combination with INH, DTT was effective at sterilizing cultures at just half the concentration used for cysteine (2 mM) (Fig. S2*A*), which substantiates the crucial role of the free-thiol group as DTT possesses two free-thiol groups, whereas cysteine has only one.

The Combination of Cysteine and RIF Prevents the Emergence of RIF-Resistant Mutants. To test whether the enhancing effect of cysteine was specific to INH, *Mtb* cultures were cotreated with cysteine and two other first-line TB drugs: RIF and ethambutol (EMB). Treatment with RIF resulted in a 3- to 4-log decrease in CFU after 2 wk followed by an increase in CFU because of the emergence of RIF-resistant mutants (Fig. S1*E*). When cysteine was added in combination with RIF, a 6-log decrease in CFUs was observed. However, a different pattern was observed for EMB (Fig. S1*F*), in that EMB treatment with or without cysteine resulted in a very slow decrease in CFU and no emergence of EMB-resistant mutants was observed. The colonies obtained after 3 wk of EMB treatment were all EMB-susceptible, whereas the majority of colonies isolated after 3 wk of INH or RIF treatment were INH-resistant or RIF-resistant, respectively. These results suggested a correlation between the emergence of a drug-resistant population and the beneficial effect of adding cysteine to a drug treatment. The remainder of this report will focus mostly on cysteine as a thiol delivery agent and its effects when combined with INH.

Transcriptional Profiling Reveals That INH/Cys Triggers an Oxidative Process. To investigate the mechanisms involved in the INH/Cys effect on *Mtb*, we performed transcriptional profiling of *Mtb* H37Rv cultures treated for 4 h with INH or with INH/Cys. The comparison of treatment with INH/Cys to INH alone revealed an up-regulation (>twofold) of 143 genes, including many involved in the conservation of cation homeostasis (genes involved in the IdeR and Zur regulon, the regulatory genes *furA* and *csoR*) (Fig. 2 and Table S2). The DosR regulon, which is induced in a *csoR* knockout strain (11), was broadly induced, as was the DNA damage response stimulon (12). INH/Cys treatment led to the up-regulation of many genes observed to be induced in *Mtb* exposed to oxidative and nitrosative stresses (13, 14). INH/Cys treatment also repressed the expression of 79 genes (>twofold), several of which are involved in intermediary metabolism and respiration as well as cation transport (Table S3). Interestingly, although the zinc uptake regulator *zur* was down-regulated, its regulon was induced (11). These data suggested that the INH/Cys combination initiated a cation-dependent oxidative stress resulting in DNA damage.

Cysteine Is Rapidly Oxidized into Cystine Leading to ROS Production. High levels of intracellular cysteine have been shown to induce ROS production leading to DNA damage and oxidation of cysteine to cystine in *Escherichia coli* (15). To test whether oxidation of cysteine occurs in the cell cytoplasm or in the supernatant of *Mtb* cultures following addition of 4 mM cysteine, the free-thiol levels were measured in cultures treated with cysteine, INH, and INH/Cys. No increase in free thiols in the cell pellets was observed up to 24 h after the addition of cysteine (Fig. 3*A*). The thiol levels were further measured over the course of 4 d of treatment, and no significant difference in cell pellet thiol content was observed. In the supernatant of these cultures, the increase in free-thiol content was transient, lasting no more than 1 h after cysteine addition (Fig. 3*B*). We then tested whether cysteine was oxidized to cystine by

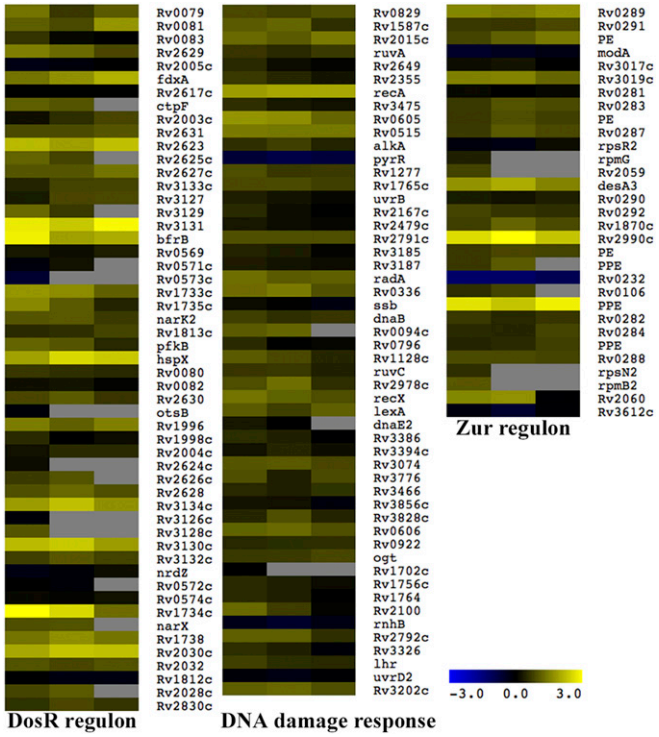

Fig. 2. Addition of cysteine to INH induces transcriptional responses to maintain cation homeostasis, counter oxidative, and genotoxic stresses. The transcriptional profile of *Mtb* H37Rv exposed for 4 h to the combination of INH (7.3 μM) and cysteine (4.0 mM) was compared with that of cells exposed to INH alone. Genes comprising the DosR regulon (35) (*Left*) were largely up-regulated in the cysteine-treated cells. The DNA damage response (12) was up-regulated (*Center*), except for the *pyrR* repressor. Likewise, the Zur regulon (11) was induced (*Right*), except for the putative repressor *Rv0232*, highlighting the effect of the cysteine treatment on cation homeostasis. Scale represents $\log_2$ fold-change vs. INH alone; cells represent biological triplicate comparisons.

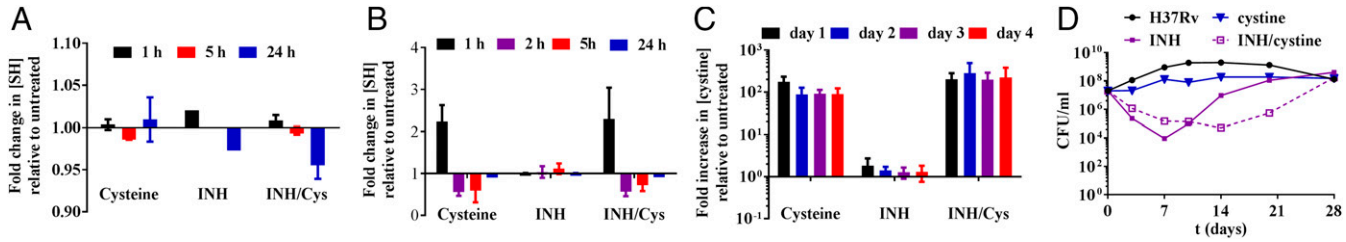

Fig. 3. High levels of cystine but not cysteine are found in *Mtb* treated with cysteine or INH/Cys. Total thiol concentrations from cell pellets (*A*) or supernatants (*B*) of *Mtb* mc^{2}6230 cultures treated with cysteine (4.0 mM), INH (7.3 μM), or INH/Cys were measured. (*C*) UPLC-MS determination of the relative amount of cystine in the cell pellets of *Mtb* mc^{2}6230 treated with cysteine (4.0 mM), INH (7.3 μM), or INH/Cys compared with pellets from untreated cells. (*D*) *Mtb* was treated with cystine (2.0 mM), INH (7.3 μM), or the combination. Aliquots were taken at indicated times and plated to determine CFUs. The combination used the same concentrations as the individual treatments. Average with SD is plotted (n = 3).

analyzing the lysates of cell pellets by liquid chromatography coupled to a mass spectrometer (UPLC-MS). Cultures treated with cysteine, with or without INH, contained at least 100-fold more cystine in their cell pellets than did the cultures that did not receive cysteine (Fig. 3*C*). Because the oxidation of cysteine to cystine occurred rapidly in the cell pellet, the sterilization effect of the INH/Cys combination might result from cystine generation in situ. Viability of *Mtb* cultures treated with INH or cystine was therefore determined to assess whether cystine was the molecule responsible for sterilization by the INH/Cys combination (Fig. 3*D*). Although a growing bacterial population emerged more slowly in *Mtb* cultures cotreated with INH and cystine, we did not observe culture sterilization, and therefore cystine is not responsible for the bactericidal activity of the INH/Cys combination.

Transition metals, such as copper or iron, are known to catalyze the oxidation of cysteine into cystine, leading to the production of hydrogen peroxide (H_2O_2), superoxide, and hydroxyl radicals (16). We hypothesized that high concentrations of cysteine could trigger a cationic stress, which could result in the formation of ROS and DNA damage (17, 18). Based on our transcriptional data indicating the possible involvement of cations in the INH/Cys combination activity, we first tested whether a cation scavenger, such as the iron chelator deferoxamine (DFO), could impair culture sterilization by INH/Cys. The addition of DFO to INH/Cys-treated *Mtb* cultures resulted in viability curves similar to those of INH-treated cultures, with the emergence of a growing population within 14 d of treatment (Fig. S3*A*). Iron is also implicated in the production of ROS by the Harber–Weiss and Fenton reactions, which rely on the reduction of ferric ions to ferrous ions in the presence of oxygen and a reductant such as cysteine. Thus, we compared the levels of free ferrous and ferric ions in *Mtb* cultures treated with cysteine, INH, and INH/Cys during a period of 2 d (Fig. S3 *B* and *C*). An increase in the ferrous ion levels was observed immediately in the cell pellet and supernatant of the INH/Cys-treated *Mtb* cultures, but the levels quickly returned to untreated levels. Interestingly, an increase in ferrous levels was subsequently observed after 24 h of treatment in both the INH/Cys and INH cell pellets. Next, superoxide levels and DNA breaks were measured in *Mtb* cultures treated with cysteine, INH, and INH/Cys during a period of 7 d by quantification using flow cytometry. Although INH/Cys treatment resulted in a clear increase in ROS formation in the first 24 h compared with treatment with cysteine or INH alone, the differences were less pronounced at later time points (Fig. 4*A*). However, this increase in ROS production correlated with a striking increase (up to 60%) in the level of double-stranded DNA breaks in the INH/Cys-treated samples after 7 d (Fig. 4*B*).

To evaluate the association between enhanced ROS production with the INH/Cys and bactericidal activity, *Mtb* was treated with cysteine, RIF, and RIF/Cys in an anaerobic chamber. For this experiment, RIF was chosen because it retains bactericidal activity under anaerobic conditions, whereas INH does not (19). Under anaerobic conditions, the addition of cysteine to RIF-treated *Mtb* did not further increase killing of the bacterial population (Fig. S3*D*), indicating an oxygen-dependent etiology. These data suggests that the sterilization phenomenon observed in INH/Cys-treated *Mtb* cultures relies on the presence of cations, such as ferric ions, and oxygen, and leads to an oxidative process and DNA damage.

The INH/Cys Combination Generates a Transient Increase in H_2O_2 Concentration. Autoxidation of 4 mM cysteine into cystine significantly increased H_2O_2 production in pig kidney cells (20). To assess whether H_2O_2 was generated concomitant with the oxidation of cysteine to cystine in *Mtb*, the concentration of H_2O_2 was measured in cultures treated with INH and/or cysteine. An increase in H_2O_2 was observed in the cultures receiving cysteine during the first 24 h of treatment: intracellular H_2O_2 levels were 1.5 and 6 times higher (Fig. 5*A*) and extracellular H_2O_2 levels were 12 and 28 times higher (Fig. 5*B*) in *Mtb* cultures treated with cysteine and INH/Cys, respectively, compared with untreated. The levels of H_2O_2 then decreased drastically after 24 h. To test whether the H_2O_2 burst was responsible for the INH/Cys sterilization effect, cultures were treated with a noninhibitory concentration of H_2O_2 (1 mM) with and without INH. No change in the growth kinetics of *Mtb* was observed in the presence of INH and H_2O_2 (Fig. S4 *A* and *B*), and a growing bacterial population emerged within 14 d of INH treatment, whether or not H_2O_2 was added to the cultures. To test whether the production of H_2O_2 and oxidation of cysteine could cause a redox unbalance, we measured the levels of NADH and NAD^+ cofactors to assess whether the cell redox potential was changed upon addition of INH/Cys and found no significant changes over time (Fig. S4*C*). These results indicate that an oxidation process leading to H_2O_2 production does occur but that it may not be the primary factor in cell death.

The INH/Cys Combination Increases *Mtb* Cellular Respiration and Prevents the Emergence of INH Persisters. Recently, a correlation between antibiotic bactericidal activity and bacterial cellular respiration

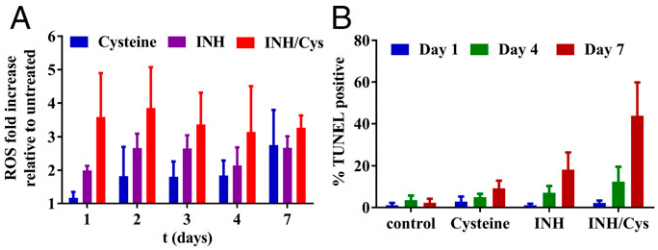

Fig. 4. The combination INH/Cys increases intracellular ROS production and DNA damage. (*A*) Cell pellets of *Mtb* mc^{2}6230 treated with INH (7.3 μM), cysteine (4.0 mM), or a combination of these using the same concentrations as the individual treatments, were stained with dihydroethidium. ROS levels were measured by flow cytometry for up to 7 d and compared with the untreated samples. (*B*) The samples in *A* were also used to determine the percentage of double-stranded DNA breakage. Average with SD is plotted (n = 3).

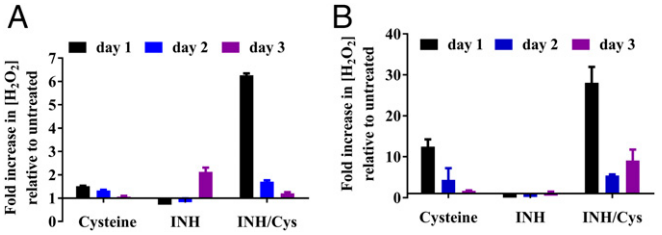

Fig. 5. The combination of cysteine and INH transiently increases H_2O_2 levels. *Mtb* mc^{2}6230 was treated with cysteine (4.0 mM), INH (7.3 μM), alone or in combination, for 3 d at 37 °C. The combination used the same concentrations as the individual treatments. H_2O_2 concentration was determined in the cell pellet (*A*) and the supernatant (*B*) of the treated cells as described in the experimental section. Average with SD is shown (n = 2).

was established (21) through the observation that bacterial respiration increased in *E. coli* and *Staphylococcus aureus* following treatment with bactericidal drugs, whereas bacteriostatic drugs resulted in respiration arrest. Previously, we had shown that the addition of high concentrations (1–40 mM) of the thiol DTT induced oxygen consumption in nonrespiring *Mtb* cells (22). Because DTT in combination with INH sterilizes *Mtb* cultures similarly to the INH/Cys combination (Fig. S2*A*), we examined whether cysteine could also increase oxygen consumption of nonrespiring *Mtb* cells. *Mtb* cultures were grown to late stationary phase where minimal oxygen consumption was observed (Fig. 6*A*). The addition of cysteine to these nonrespiring cells had a modest effect on respiration, but the addition of INH/Cys provoked a rapid resumption of oxygen consumption (Fig. 6*A*).

The stimulation of respiration by DTT in cells with previously reduced oxygen consumption was shown to be because of an increase in the menaquinol-9 (MKH_2) pool, which controls *Mtb* respiratory rate (22). We observed that the combination of INH/Cys further increases *Mtb* respiration above the increase generated by cysteine alone, suggesting a similar mechanism whereby the addition of high concentrations of cysteine shifts the ratio of MKH_2 to menaquinone-9 (MK) toward higher MKH_2 levels, resulting in enhanced bacterial respiration. To test this hypothesis, MK and MKH_2 were extracted from *Mtb* cultures treated with INH, cysteine, and INH/Cys, and analyzed by UPLC-MS (Fig. S5*A*). The addition of INH/Cys had the greatest impact on the MKH_2/MK ratio, with an increase up to 13 times that of untreated cells. This increase in the MKH_2/MK ratio occurred within the first 3 h of treatment, followed by a steady decrease over time.

Finally, we use the dual GFP/RFP-reporter mycobacteriophage Φ^2DRM9 (10) to assess the effects of INH/Cys on metabolic rate and persister formation in *Mtb*. Expression level of GFP and RFP in *Mtb* infected with Φ^2DRM9 depends on the metabolic status of the infecting cell. Actively growing cells express a higher level of GFP and a lower level of RFP in >90% of *Mtb* (Fig. S6). In contrast, INH persisters are characterized by low GFP/high RFP fluorescence after Φ^2DRM9 infection (10). *Mtb* cultures treated with cysteine, INH, or INH/Cys for up to 4 d were infected with Φ^2DRM9 (Fig. S6). Both microscopy and flow cytometry analysis showed the presence of the persister population (low GFP/high RFP) in the INH-treated samples at the end of day 4 (Fig. 6 *B* and *C* and Fig. S6). In contrast, this population was missing in the INH/Cys-treated samples (Fig. 6 *B* and *C* and Fig. S6). Furthermore, the INH/Cys-treated sample had a relatively greater population of cells expressing high GFP signal than the INH-treated samples, suggesting a higher metabolic rate of *Mtb* in this sample. These findings are consistent with a model in which a shift toward higher MKH_2 levels increases the *Mtb* respiratory rate and thus prevents cells from entering a persister or drug-tolerant state.

The INH/Cys Combination Potentiates INH Activity in Macrophages. *Mtb* is an intracellular pathogen that infects host macrophages, and so to be effective, a drug or drug combination needs to be transported through both the macrophage membrane and the mycobacterial cell wall. To assess whether the addition of a thiol to INH treatment would improve TB chemotherapy, we tested the combination of INH/thiol in *Mtb*-infected J774 murine macrophages. First, the cytotoxicity of cysteine for the host cells was determined, and the highest concentration of cysteine that allowed for at least 90% survival (LC_{10}) of macrophages was 0.0156 mM. In contrast, the thiol *N*-acetylcysteine (NAC) had an LC_{10} of 5–10 mM in J774 macrophages and, in *Mtb* in vitro cultures, led to a 4- to 5-log decrease in CFUs within 3 wk when combined with INH (Fig. S2*B*). *Mtb*-infected macrophages were treated with NAC in combination with INH for 7 d (Fig. 7*A*). Although NAC did not impair the growth of *Mtb* in J774 macrophages, INH/NAC was significantly more effective at killing intracellular *Mtb* than INH alone (Fig. 7*B*). These observations demonstrate that the addition of NAC can enhance chemotherapy of *Mtb* in mammalian cells.

Discussion

Several mechanisms potentially underlie the sterilizing activity of the INH/Cys combination. The transcriptional data suggested mechanisms based on oxidative stress leading to DNA damage. Indeed, we showed that ROS concentrations were higher in INH/Cys-treated *Mtb* leading to DNA damage, which correlates with

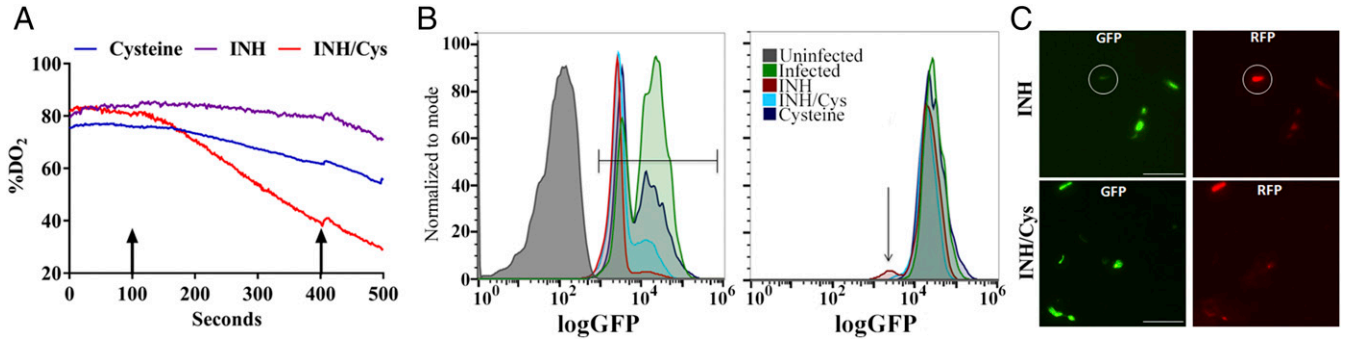

Fig. 6. INH/Cys induces *Mtb* respiration and prevents persister formation. (*A*) The levels of dissolved oxygen (DO_2) in *Mtb* were followed upon treatment with cysteine (4.0 mM), INH (7.3 μM), and INH/Cys. The first 100 s show the oxygen consumption of *Mtb* mc^{2}6230 in stationary phase. Compounds were added at 100 s (left arrow), followed at 400 seconds (right arrow) by the addition of the respiration uncoupler CCCP. The curves represent a typical experiment from biological triplicates. (*B*) Four-day-old *Mtb* cultures treated with cysteine (4.0 mM), INH (7.3 μM), and INH/Cys (7.3 μM/4.0 mM) were infected with Φ^2DRM9 and analyzed by flow cytometry. GFP expression after phage infection represents viable *Mtb* cells with higher GFP$^+$ cells being more metabolically active (*Left*). The RFP population was back-gated to show GFP expression distribution in these cells (*Right*). The low-GFP/high-RFP (persister) population indicated by an arrow was absent in the INH/Cys-treated *Mtb* cultures (*Right*). (*C*) Representative microscopy images showing the presence and absence of persisters (low GFP/high RFP) in INH- (*Upper*) and INH/Cys-treated (*Lower*) *Mtb* cultures, respectively. (Scale bar, 10 μm.)

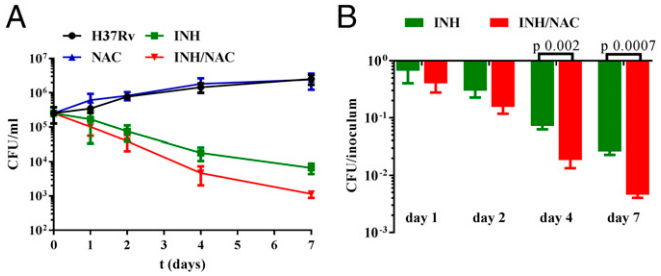

Fig. 7. The combination of INH and NAC increases the intracellular killing of *Mtb* in murine macrophages. (*A*) J774 macrophages were infected with *Mtb* H37Rv at an MOI of 1 for 4 h before treatment with NAC (2.0 mM), INH (7.3 μM), or their combination at the same concentrations. (*B*) Intracellular *Mtb* killing upon treatment is represented by plotting bacterial load against titer at beginning of treatment. *P* was determined by two-tailed student's test. Average with SD is shown ($n = 4$).

previously published work showing that high concentrations of intracellular cysteine increased DNA damage in *E. coli* (15). The lack of RIF/Cys activity under anaerobic conditions further suggests that oxygen plays an important role in our observed phenomenon. Furthermore, the increase in intracellular cystine concentration with no commensurate increase in cysteine concentration in the cysteine-treated cultures also points to an oxidative process, although cystine was not a key player in the sterilization phenotype. Although several lines of inquiries point to an oxidative process, the addition of a specific oxidant, H_2O_2, to INH-treated *Mtb* cultures did not mimic the sterilizing effect of INH/Cys in vitro.

Combining cysteine with INH treatment of exponentially growing *Mtb* cells prevented the emergence of drug-resistant mutants and ultimately led to sterilization of the cultures. Interestingly, this combination did not work when cysteine was added 2 d or more after the addition of INH to the *Mtb* cultures, implying that INH/Cys might prevent the formation of the persister population, which is often associated with treatment failure and the emergence of a drug-resistant population in TB-infected patients. Previously, the generation of INH persisters in *Mtb* cultures was associated with random on/off expression of the catalase/peroxidase KatG, the activator of INH (23). Those authors hypothesized that *Mtb* cells might alter KatG expression in response to ROS fluctuation during active respiratory metabolism. In our study, we observed a consistently higher ROS production in the INH/Cys-treated samples than in INH-treated samples, as well as up-regulation of *katG* (> fourfold). This finding suggests that higher respiratory metabolism leads to increased ROS production and KatG expression as a compensatory mechanism, which might result in enhanced INH activity and ultimately *Mtb* cell death. The mycobacterial persister population was also shown to be sensitive to oxygen concentration and could be killed at higher concentrations of dissolved oxygen that led to ROS production and sterilization of the culture (24). In our study, the persister population was absent in the INH/Cys-treated *Mtb* culture, suggesting that conditions or compounds that increase oxygen consumption would lead to the depletion of persister cells or the prevention of their appearance, which ultimately would result in sterilization of drug-treated *Mtb* cultures. Notably, vitamin C, which we had showed sterilized *Mtb* cultures (25), was also found to induce *Mtb* respiration (Fig. S5*B*), suggesting that this mechanism is not specific to the combination of thiols and INH.

NAC showed a similar sterilizing effect to cysteine when combined with INH in vitro (Fig. S2*B*). Recently, it was shown that when NAC was added to *Mtb* treated with the combination of electron transport chain inhibitors bedaquiline, Q203, and clofazimine, no colony could be detected after 5 d of treatment (26). In murine macrophages, INH/NAC reduced intracellular *Mtb* growth significantly better than INH alone (Fig. 7). NAC (10 mM) was also found to have moderate antimycobacterial activity in human THP-1 macrophages, resulting in a threefold decrease in bacterial load after 5 d (27). In the same study, the authors also showed that NAC was safe in mice and a dose of 400 mg/kg given by gavage daily to *Mtb*-infected mice could by itself reduce the mycobacterial lung burden by half a log (27). This result suggests that combining NAC to first-line TB drugs could further decrease organ bacterial loads in *Mtb*-infected mice and should be investigated. Furthermore, NAC is used for the treatment of drug-induced toxicity in TB patients (28, 29) and, when tested as an adjuvant to directly observed treatment short course, NAC significantly caused early sputum negativity and radiological improvement in pulmonary TB patients (30). Along with the increased bactericidal activity of the INH/NAC combination in our murine macrophage model, these data suggest that NAC could potentiate the efficacy of TB chemotherapy.

We show that INH/Cys enhances *Mtb* oxygen consumption. We propose that INH/Cys works by preventing *Mtb* from entering a low respiratory and low metabolic state, which might be found in persisters, and allows bactericidal drugs such as INH to continue to exert their activity. Furthermore, without persisters there is no opportunity for mutagenesis leading to the emergence of drug resistance. A consequence of increased oxygen consumption may be the generation of ROS, which was observed in the INH/Cys-treated *Mtb* cultures, and which might contribute to the enhanced bactericidal activity of the INH/Cys combination (Fig. S7). We have previously demonstrated that respiration can be controlled by the poise of the menaquinone/menaquinol pool and that respiration is inhibited when the pool is in an oxidized state (22). Here, we show that the addition of cysteine to INH-treated *Mtb* cultures shifts the pool toward a reduced state and allows *Mtb* cells that were not respiring to resume respiration. This finding is in accordance with our transcriptional data, which showed up-regulation of the DosR regulon, which enhances the emergence of *Mtb* from nonrespiring dormancy (31). This effect on the DosR regulon might also be a consequence of the reduction of copper by cysteine, which can lead to the generation of nitric oxide that activates the sensor histidine kinases DosS and DosT (32, 33). In conclusion, we suggest that the control of respiration via the menaquinol pool is a key step in fostering drug tolerance and drug resistance in *Mtb*. Moreover, considering the increasing incidence of MDR- and XDR-TB, new strategies to treat resistant infections and prevent the emergence of resistance are urgently needed; the addition of nontoxic, small molecules, such as NAC to TB chemotherapy, presents a promising approach to these chemotherapeutic challenges in the treatment of TB, warranting further study.

Materials and Methods

Bacterial Strains and Reagents. The *Mtb* strains used in this study and the phage Φ^2DRM9 were obtained from laboratory stocks. The *Mtb* strains were grow at 37 °C while shaking in Middlebrook 7H9 medium (Difco) supplemented with 10% (vol/vol) OADC enrichment (oleic acid-albumin-dextrose-catalase, Difco), 0.2% (vol/vol) glycerol, and 0.05% (vol/vol) tyloxapol. The solid media used was Middlebrook 7H10 medium (Difco) supplemented with 10% (vol/vol) OADC enrichment (Difco) and 0.2% (vol/vol) glycerol. Plates were incubated at 37 °C for up to 6 wk. For safety purposes, specific experiments were performed with *Mtb* $mc^2$6230, a nonpathogenic deletion mutant (ΔRD1 Δ*panCD*) of strain H37Rv that can safely be used in a Biosafety Level 2 laboratory. To culture $mc^2$6230, *D*-pantothenic acid hemicalcium salt (25 mg/L) was added to liquid and solid media. All chemicals were obtained from Sigma unless otherwise stated. All solvents used were LC-MS grade (Fisher).

Growth of *Mtb* in Vitro Cultures. *Mtb* cultures were grown at 37 °C to an optical density at 600 nm (OD_{600nm}) of 0.7–1.0. The cultures were diluted 1/50, treated with the appropriate chemicals, and incubated at 37 °C with shaking for the duration of the experiment. The addition of 4 mM of cysteine to *Mtb* cultures did not change the pH of the cultures. The OD_{600nm} was recorded, and CFUs were obtained by plating serial dilutions (see media described above).

Determination of Total Thiol Concentration. An exponentially growing *Mtb* mc^2 6230 culture was diluted to an $OD_{600nm} \sim 0.15$, treated with the appropriate chemicals, and incubated at 37 °C while shaking. The cultures (10 mL) were centrifuged, and the cell pellets were washed once with PBS and resuspended in 50 mM Tris (pH 8.0; 0.5 mL) containing 5 mM EDTA. Glass beads (0.1 mm diameter, 0.1 mL) were added, and the cell pellets were lysed using the MP Bio FastPrep machine (45 s, speed 6 M/s, three times). After cooling, the samples were

centrifuged and the supernatants were filter-sterilized before analysis. The total thiol concentration was obtained by measuring spectrophotometrically at 412 nm a 1-mL solution containing 50 mM Tris (pH 8.0), 5 mM 5,5′-dithiobis(2-nitrobenzoic acid) (10 μL), and the sample lysate using the following extinction coefficient: $\varepsilon_{412\ nm}$ 2-nitro-5-thiobenzoate anion 14,150 $M^{-1}{\cdot}cm^{-1}$.

ROS and DNA Breaks Analyses. *Mtb* mc^{2}6230 was grown to OD_{600nm} 1.0 and diluted to an OD_{600nm} of 0.2 in fresh media containing the appropriate chemicals. For ROS analysis, aliquots were taken at the indicated time points, and cells were stained with dihydroethidium (5 μM) for 30 min at 37 °C and immediately analyzed on a BD FACS Calibur (BD Biosciences) as described previously (25). Aliquots from the same mycobacterial cells used for ROS analysis were removed at indicated time points, fixed, treated with TUNEL reaction mix from the In Situ Cell Death Detection Kit (Roche Molecular Biochemicals), and analyzed by flow cytometry, as described previously (25).

Determination of Oxygen Consumption. The oxygen consumption rate was determined using a Clark-type oxygen electrode (Rank Brothers) linked to an ADC-24 data logger (Pico Technology). *Mtb* mc^{2}6230 was grown to stationary phase and 5 mL were added to the incubation chamber to measure basal level oxygen consumption. After 100 s, cysteine, INH, or INH/Cys was added at the indicated concentration, and oxygen consumption was recorded for another 300 s, after which maximal uncoupled respiration was measured with the addition of carbonyl cyanide 3-chlorophenylhydrazone (CCCP, 200 nmol) for 100 s.

J774 Murine Macrophage Experiments. J774A.1 macrophages (ATCC) were subcultured twice a week according to the supplier's recommendations in DMEM (Invitrogen), supplemented with 10% FBS (Invitrogen). Cell viability was assessed using the MTT assay (34). For the infection assays, the macrophages (~100,000 cells) were seeded into each chamber of a 24-well tissue culture plate and cultured for 3 d. At the time of the infection, cell density was ~3.5×10^5 cells per well. For the infection, a *Mtb* H37Rv culture was grown to midlog (OD_{600nm} ~ 0.6–0.8), washed twice in PBS supplemented with 0.05% tyloxapol, resuspended in PBS, and sonicated twice for 10 s. The culture was then diluted in DMEM supplemented with 10% FBS and used to infect the J774 cells for 4 h at 37 °C in 5% CO_2 at an approximate multiplicity of infection (MOI) of 1 to allow for bacterial uptake. Cell monolayers were then washed twice with PBS, and cultured in DMEM supplemented with 10% FBS and the appropriate test compounds, while incubating at 37 °C in 5% CO_2. The media with compounds was replenished at days 2 and 4. At each time point, the media was removed from the wells; the wells were washed once with PBS and then treated for 5 min with 0.05% aqueous SDS solution to lyse the macrophages. The lysates were serially diluted and plated for CFU determination.

Additional methods are available in *SI Materials and Methods*.

ACKNOWLEDGMENTS. W.R.J. acknowledges generous support from the NIH Centers for AIDS Research Grant (CFAR) AI-051519 at the Albert Einstein College of Medicine. This work was supported by the National Institutes of Health Grants AI26170 and U19AI111276 (to W.R.J.), Potts Memorial Foundation research grant (to P.J.), and Stony Wold-Herbert foundation (P.J.).

1. Raviglione M, Sulis G (2016) Tuberculosis 2015: Burden, challenges and strategy for control and elimination. *Infect Dis Rep* 8:6570.
2. Zhang Y, Heym B, Allen B, Young D, Cole S (1992) The catalase-peroxidase gene and isoniazid resistance of *Mycobacterium tuberculosis*. *Nature* 358:591–593.
3. Vilchèze C, Jacobs WR, Jr (2014) Resistance to isoniazid and ethionamide in *Mycobacterium tuberculosis*: Genes, mutations, and causalities. *Microbiol Spectr* 2:MGM2-0014-2013.
4. Ung KS, Av-Gay Y (2006) Mycothiol-dependent mycobacterial response to oxidative stress. *FEBS Lett* 580:2712–2716.
5. Buchmeier NA, Newton GL, Koledin T, Fahey RC (2003) Association of mycothiol with protection of *Mycobacterium tuberculosis* from toxic oxidants and antibiotics. *Mol Microbiol* 47:1723–1732.
6. Newton GL, et al. (1999) Characterization of *Mycobacterium smegmatis* mutants defective in 1-*d*-myo-inosityl-2-amino-2-deoxy-alpha-*d*-glucopyranoside and mycothiol biosynthesis. *Biochem Biophys Res Commun* 255:239–244.
7. Rawat M, et al. (2002) Mycothiol-deficient *Mycobacterium smegmatis* mutants are hypersensitive to alkylating agents, free radicals, and antibiotics. *Antimicrob Agents Chemother* 46:3348–3355.
8. Vilchèze C, et al. (2011) Coresistance to isoniazid and ethionamide maps to mycothiol biosynthetic genes in *Mycobacterium bovis*. *Antimicrob Agents Chemother* 55: 4422–4423.
9. Vilchèze C, et al. (2008) Mycothiol biosynthesis is essential for ethionamide susceptibility in *Mycobacterium tuberculosis*. *Mol Microbiol* 69:1316–1329.
10. Jain P, et al. (2016) Dual-reporter mycobacteriophages (Φ^2DRMs) reveal preexisting *Mycobacterium tuberculosis* persistent cells in human sputum. *MBio* 7:e01023-16.
11. Maciag A, et al. (2007) Global analysis of the *Mycobacterium tuberculosis* Zur (FurB) regulon. *J Bacteriol* 189:730–740.
12. Boshoff HI, et al. (2004) The transcriptional responses of *Mycobacterium tuberculosis* to inhibitors of metabolism: Novel insights into drug mechanisms of action. *J Biol Chem* 279:40174–40184.
13. Voskuil MI, et al. (2003) Inhibition of respiration by nitric oxide induces a *Mycobacterium tuberculosis* dormancy program. *J Exp Med* 198:705–713.
14. Schnappinger D, et al. (2003) Transcriptional adaptation of *Mycobacterium tuberculosis* within macrophages: Insights into the phagosomal environment. *J Exp Med* 198: 693–704.
15. Park S, Imlay JA (2003) High levels of intracellular cysteine promote oxidative DNA damage by driving the fenton reaction. *J Bacteriol* 185:1942–1950.
16. Kachur AV, Koch CJ, Biaglow JE (1999) Mechanism of copper-catalyzed autoxidation of cysteine. *Free Radic Res* 31:23–34.
17. Demple B, Harrison L (1994) Repair of oxidative damage to DNA: Enzymology and biology. *Annu Rev Biochem* 63:915–948.
18. Imlay JA, Chin SM, Linn S (1988) Toxic DNA damage by hydrogen peroxide through the Fenton reaction in vivo and in vitro. *Science* 240:640–642.
19. Piccaro G, Giannoni F, Filippini P, Mustazzolu A, Fattorini L (2013) Activities of drug combinations against *Mycobacterium tuberculosis* grown in aerobic and hypoxic acidic conditions. *Antimicrob Agents Chemother* 57:1428–1433.
20. Nath KA, Salahudeen AK (1993) Autoxidation of cysteine generates hydrogen peroxide: Cytotoxicity and attenuation by pyruvate. *Am J Physiol* 264:F306–F314.
21. Lobritz MA, et al. (2015) Antibiotic efficacy is linked to bacterial cellular respiration. *Proc Natl Acad Sci USA* 112:8173–8180.
22. Hartman T, et al. (2014) Succinate dehydrogenase is the regulator of respiration in *Mycobacterium tuberculosis*. *PLoS Pathog* 10:e1004510.
23. Wakamoto Y, et al. (2013) Dynamic persistence of antibiotic-stressed mycobacteria. *Science* 339:91–95.
24. Grant SS, Kaufmann BB, Chand NS, Haseley N, Hung DT (2012) Eradication of bacterial persisters with antibiotic-generated hydroxyl radicals. *Proc Natl Acad Sci USA* 109: 12147–12152.
25. Vilchèze C, Hartman T, Weinrick B, Jacobs WR, Jr (2013) *Mycobacterium tuberculosis* is extraordinarily sensitive to killing by a vitamin C-induced Fenton reaction. *Nat Commun* 4:1881.
26. Lamprecht DA, et al. (2016) Turning the respiratory flexibility of *Mycobacterium tuberculosis* against itself. *Nat Commun* 7:12393.
27. Amaral EP, et al. (2016) N-acetyl-cysteine exhibits potent anti-mycobacterial activity in addition to its known anti-oxidative functions. *BMC Microbiol* 16:251.
28. Baniasadi S, et al. (2010) Protective effect of *N*-acetylcysteine on antituberculosis drug-induced hepatotoxicity. *Eur J Gastroenterol Hepatol* 22:1235–1238.
29. Kranzer K, et al. (2015) A systematic review and meta-analysis of the efficacy and safety of *N*-acetylcysteine in preventing aminoglycoside-induced ototoxicity: Implications for the treatment of multidrug-resistant TB. *Thorax* 70:1070–1077.
30. Dinesh N, Sunil M, Sanjay G (2013) Supplementation of N-acetylcysteine as an adjuvant in treatment of newly diagnosed pulmonary tuberculosis patients: A prospective, randomized double blind, placebo controlled study. *Eur Respir J* 42:P2833.
31. Leistikow RL, et al. (2010) The *Mycobacterium tuberculosis* DosR regulon assists in metabolic homeostasis and enables rapid recovery from nonrespiring dormancy. *J Bacteriol* 192:1662–1670.
32. Marcus SA, Sidiropoulos SW, Steinberg H, Talaat AM (2016) CsoR is essential for maintaining copper homeostasis in *Mycobacterium tuberculosis*. *PLoS One* 11:e0151816.
33. Dicks AP, Williams DL (1996) Generation of nitric oxide from S-nitrosothiols using protein-bound Cu2+ sources. *Chem Biol* 3:655–659.
34. Mosmann T (1983) Rapid colorimetric assay for cellular growth and survival: Application to proliferation and cytotoxicity assays. *J Immunol Methods* 65:55–63.
35. Park HD, et al. (2003) Rv3133c/dosR is a transcription factor that mediates the hypoxic response of *Mycobacterium tuberculosis*. *Mol Microbiol* 48:833–843.